

# When is the Resolvent Like a Rank One Matrix?

Anne Greenbaum\*, Faranges Kyanfar†, Abbas Salemi‡

January 15, 2025

## Abstract

For a square matrix  $A$ , the resolvent of  $A$  at a point  $z \in \mathbb{C}$  is defined as  $(A - zI)^{-1}$ . We consider the set of points  $z \in \mathbb{C}$  where the relative difference in 2-norm between the resolvent and the nearest rank one matrix is less than a given number  $\epsilon \in (0, 1)$ . We establish a relationship between this set and the  $\epsilon$ -pseudospectrum of  $A$ , and we derive specific results about this set for Jordan blocks and for a class of large Toeplitz matrices. We also derive disks about the eigenvalues of  $A$  that are contained in this set, and this leads to some new results on disks about the eigenvalues that are contained in the  $\epsilon$ -pseudospectrum of  $A$ . In addition, we consider the set of points  $z \in \mathbb{C}$  where the absolute value of the inner product of the left and right singular vectors corresponding to the largest singular value of the resolvent is less than  $\epsilon$ . We demonstrate numerically that this set can be almost as large as the one where the relative difference between the resolvent and the nearest rank one matrix is less than  $\epsilon$  and we give a partial explanation for this. Some possible applications are discussed.

## 1 Introduction

Let  $A$  be an  $n$  by  $n$  matrix,  $n \geq 2$ . The *resolvent* of  $A$  at a point  $z \in \mathbb{C}$  is defined as  $(A - zI)^{-1}$ . If the singular values of  $(A - zI)^{-1}$  are denoted as  $\sigma_1(z) \geq \dots \geq \sigma_n(z)$ , and the corresponding left and right singular vectors are  $u_j(z)$  and  $v_j(z)$ ,  $j = 1, \dots, n$ , then the nearest rank one matrix to  $(A - zI)^{-1}$  in the 2-norm is  $\sigma_1(z)u_1(z)v_1(z)^H$ , and the 2-norm of the difference between the resolvent and this rank one matrix is  $\sigma_2(z)$ . The *relative difference* in 2-norm between the resolvent and this rank one matrix can be defined as

$$\|(A - zI)^{-1} - \sigma_1(z)u_1(z)v_1(z)^H\|_2 / \|(A - zI)^{-1}\|_2 = \sigma_2(z)/\sigma_1(z). \quad (1)$$

We are interested in the set  $S_\epsilon(A)$  where this relative difference is less than a given  $\epsilon \in (0, 1)$ :

$$S_\epsilon(A) := \{z \in \mathbb{C} : \sigma_2(z)/\sigma_1(z) < \epsilon\}. \quad (2)$$

If  $z$  is an eigenvalue of  $A$ , we will define the ratio in (2) to be 0, so the spectrum of  $A$  is always included in  $S_\epsilon(A)$ . If  $A$  is a multiple of the identity, then this is all that is included in  $S_\epsilon(A)$ .

The following theorem lists some simple properties of  $S_\epsilon(A)$ .

**Theorem 1.** *Let  $A$  be a square matrix and let  $S_\epsilon(A)$  be defined by (2) for  $\epsilon \in (0, 1)$ . Then:*

1. *For any constant  $c$ ,  $S_\epsilon(A + cI) = c + S_\epsilon(A)$ .*

---

\*University of Washington, Applied Math Dept., Box 353925, Seattle, WA 98195. email: greenbau@uw.edu

†Shahid Bahonar University of Kerman, Applied Math Dept., Kerman, Iran. kyanfar@uk.ac.ir

‡Mahani Math Center, Afzalipour Research Institute, Shahid Bahonar University of Kerman, Kerman, Iran. salemi@uk.ac.ir

2. For any constant  $c$ ,  $S_\epsilon(cA) = cS_\epsilon(A)$ .
3.  $S_\epsilon(A^H) = \overline{S_\epsilon(A)}$ .
4. For any unitary matrix  $Q$ ,  $S_\epsilon(Q^H A Q) = S_\epsilon(A)$ .
5.  $S_\epsilon(A)$  is the set of points  $z \in \mathbb{C}$  for which the ratio of the smallest to the second smallest singular value of  $A - zI$  is less than  $\epsilon$ . (If  $A - zI$  has a zero singular value, we define this ratio to be zero, even if  $A - zI$  has more than one zero singular value.)
6. If  $A$  is block diagonal,  $A := \text{blockdiag}(A_1, \dots, A_m)$ , then  $S_\epsilon(A) \subseteq \bigcup_{j=1}^m S_\epsilon(A_j)$ . In the other direction  $S_\epsilon(A)$  contains the set of points  $z$  such that  $z \in S_\epsilon(A_k)$  for some block  $k$ , and for each  $\ell \neq k$ , the smallest singular value of  $A_\ell - zI$  is greater than or equal to the second smallest singular value of  $A_k - zI$ .

*Proof.* 1. Since  $(A - zI)^{-1} = (A + cI - (z + c)I)^{-1}$ ,  $z \in S_\epsilon(A)$  if and only if  $z + c \in S_\epsilon(A + cI)$ .

2. Since the ratio in (2) remains unchanged if  $A$  is replaced by  $cA$  and  $z$  is replaced by  $cz$ , it follows that  $S_\epsilon(cA) = cS_\epsilon(A)$ .
3. Since  $(A^H - \bar{z}I)^{-1} = ((A - zI)^{-1})^H$ , the singular values of  $(A^H - \bar{z}I)^{-1}$  are the same as those of  $(A - zI)^{-1}$ , and therefore  $\bar{z} \in S_\epsilon(A^H)$  if and only if  $z \in S_\epsilon(A)$ .
4. Since the singular values of  $(Q^H A Q - zI)^{-1} = Q^H (A - zI)^{-1} Q$  are the same as those of  $(A - zI)^{-1}$ , it follows that  $S_\epsilon(Q^H A Q) = S_\epsilon(A)$ .
5. The singular values of  $A - zI$  are the inverses of the singular values of  $(A - zI)^{-1}$ , so the ratio of the smallest to the second smallest singular value of  $A - zI$  is the same as the ratio of the second largest to the largest singular value of  $(A - zI)^{-1}$ .
6. Using result 4, the singular values of  $A - zI$  are the singular values of all of the blocks  $A_j - zI$ ,  $j = 1, \dots, m$ . Suppose the smallest singular value of  $A - zI$  is the smallest singular value of  $A_k - zI$ . The second smallest singular value of  $A - zI$  is less than or equal to the second smallest singular value of  $A_k - zI$ , so that if  $z \in S_\epsilon(A)$ , then  $z \in S_\epsilon(A_k)$ . In the other direction, if the singular values of all blocks  $A_\ell - zI$ ,  $\ell \neq k$  are all greater than or equal to the two smallest singular values of  $A_k - zI$ , then the ratio of the smallest to the second smallest singular value of  $A - zI$  is the same as that of  $A_k - zI$ , so if  $z \in S_\epsilon(A_k)$ , then  $z \in S_\epsilon(A)$ .

□

In Section 2, we present numerical examples showing that when  $A$  has ill-conditioned eigenvalues, the set  $S_\epsilon(A)$  can be large – much larger than, say, a union of disks of radius  $\epsilon$  about the eigenvalues of  $A$ .

This set clearly is related to the 2-norm  $\epsilon$ -pseudospectrum of  $A$  [15], which can be defined as

$$\Lambda_\epsilon(A) := \{z \in \mathbb{C} : 1/\sigma_1(z) < \epsilon\}. \quad (3)$$

Note a difference in scaling, however, in that, unlike property 2 in Theorem 1, it is not  $\Lambda_\epsilon(cA)$  that is equal to  $c\Lambda_\epsilon(A)$  but  $\Lambda_{|c|\epsilon}(cA) = c\Lambda_\epsilon(A)$ . The relationship between the two sets is characterized in Section 3.

Sections 4 and 5 deal with Jordan blocks and large Toeplitz matrices. For a Jordan block, we derive a disk about the eigenvalue that is contained in  $S_\epsilon(A)$ , while for more general Toeplitz

matrices, we discuss what happens when the *symbol* of the Toeplitz operator has winding number  $\pm 1$  about the origin. For any shift  $-z$  that maintains this property, we use the *splitting property* to argue that as  $n \rightarrow \infty$ , the smallest singular value of  $A - zI$  approaches 0 and the second smallest singular value approaches a nonzero value. Thus, for  $n$  sufficiently large,  $z$  will lie in  $S_\epsilon(A)$ .

Section 6 is devoted to more general diagonalizable matrices, and we again derive disks about the eigenvalues that are contained in  $S_\epsilon(A)$ . This leads to a new result about disks about the eigenvalues that are contained in the  $\epsilon$ -pseudospectrum.

It was observed in [4] that not only can  $S_\epsilon(A)$  be a large set, but that throughout much of this set it may be the case that  $|u_1(z)^H v_1(z)| < \epsilon$ . If  $z$  is extremely close to an ill-conditioned eigenvalue  $\lambda$  of  $A$  (*much* closer to  $\lambda$  than to any other eigenvalue of  $A$ ), then this is to be expected since  $u_1(z)$  and  $v_1(z)$  will be close to the unit left and right eigenvectors  $x$  and  $y$  associated with the eigenvalue  $\lambda$ ; the *condition number* of  $\lambda$  is defined as  $1/|y^H x|$ , and  $\lambda$  is said to be ill-conditioned when  $|y^H x|$  is tiny. It was observed, however, that  $u_1(z)$  and  $v_1(z)$  may be nearly orthogonal to each other even when  $z$  is too far away from any eigenvalue of  $A$  for  $u_1(z)$  and  $v_1(z)$  to resemble left and right eigenvectors. In Section 7, we give a partial explanation for this observation.

Finally, in Section 8 we mention some possible applications and remaining open problems.

Throughout the paper, superscript  $H$  denotes the complex conjugate transpose of a vector or matrix and  $\|\cdot\|$  denotes the 2-norm for vectors and the corresponding spectral norm (i.e., the largest singular value) for matrices. In this section, we have denoted the singular values of  $(A - zI)^{-1}$  as  $\sigma_j(z)$ ,  $j = 1, \dots, n$ , to emphasize the fact that  $A$  is fixed and  $\sigma_j$  varies with  $z$ , and we will retain this notation in Section 2 and in Section 8. In Section 7, we deal with matrices of the form  $A - re^{i\theta}I$ , where  $A$  and  $\theta$  are fixed, and we denote their singular values as  $\sigma_j(r)$ . Throughout most of the paper, however, we deal with a number of different matrices so we will denote the singular values of a matrix  $B$  explicitly as  $\sigma_j(B)$ .

## 2 Numerical Examples

The phenomenon described in the Introduction is illustrated in Figures 1–3 for three matrices with ill-conditioned eigenvalues – the Grcar matrix<sup>1</sup> of size  $n = 50$ , the `transient_demo` matrix<sup>2</sup> of size  $n = 50$ , and the sampling matrix<sup>3</sup> of size  $n = 10$ . For the Grcar matrix, the eigenvalue condition numbers vary from about  $1.5e+2$  to  $2.2e+7$ , with the most ill-conditioned eigenvalues being those with imaginary part near  $\pm 2$  and the best conditioned being those with real part about 1.6 and imaginary part  $\pm 1.1$  (those near where the curved sections of eigenvalues meet). All eigenvalues of the `transient_demo` matrix have the same condition number, about  $7.2e+5$ . The eigenvalues of the sampling matrix have condition numbers ranging from about  $1.4e+3$  to  $1.3e+6$ , with the interior eigenvalues being more ill-conditioned than those at the ends. The plots on the left show contours of the ratio of the second largest to the largest singular value of  $(A - zI)^{-1}$ , which, as noted previously, is the relative difference in 2-norm between  $(A - zI)^{-1}$  and the nearest rank one matrix.

The right plots in the figures show the absolute values of the inner products of the left and right singular vectors  $u_1(z)$  and  $v_1(z)$  corresponding to the largest singular value of  $(A - zI)^{-1}$ .

---

<sup>1</sup>In MATLAB, `gallery('grcar',50)`. This matrix has  $-1$ 's on the subdiagonal,  $1$ 's on the main diagonal and the first three super-diagonals, and  $0$ 's elsewhere.

<sup>2</sup>In [17], `transient_demo(50)`.

<sup>3</sup>In MATLAB, `gallery('sampling',10)`. This matrix has integer eigenvalues,  $0, 1, \dots, 9$ , that are ill-conditioned.

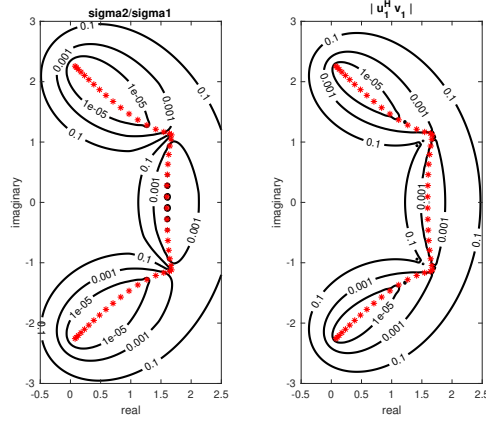


Figure 1: Contour plots of ratios of second largest to largest singular value of the resolvent (left) and of absolute value of inner product of left and right singular vectors corresponding to largest singular value of the resolvent (right). Matrix is the Grcar matrix of size  $n = 50$ . Eigenvalues are shown with red asterisks.

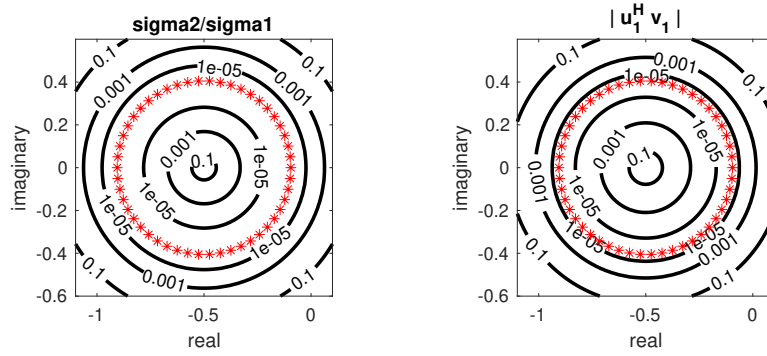


Figure 2: Contour plots of ratios of second largest to largest singular value of the resolvent (left) and of absolute value of inner product of left and right singular vectors corresponding to largest singular value of the resolvent (right). Matrix is the transient\_demo matrix of size  $n = 50$ . Eigenvalues are shown with red asterisks.

It can be seen from the figures that these inner products are small even when  $z$  is too far away from any eigenvalue to argue that  $u_1(z)$  and  $v_1(z)$  resemble unit left and right eigenvectors.

In contrast, if we take a normal matrix whose eigenvalues are the same as those of, say, the Grcar matrix, then the contours plotted in Figure 1 will not be visible on the scale of the graph; for illustration, we plot in Figure 4 the contour where  $\sigma_2(z)/\sigma_1(z) = 0.5$  for a diagonal matrix whose eigenvalues are those of the Grcar matrix. Clearly, the phenomenon illustrated in Figures 1–3 is limited to matrices with at least some ill-conditioned eigenvalues.

### 3 Relation to Pseudospectra

The  $\epsilon$ -pseudospectrum [15] of a matrix  $A$  is usually defined as

$$\{z \in \mathbb{C} : \|(A - zI)^{-1}\| > \epsilon^{-1}\}. \quad (4)$$

For the 2-norm this is clearly equivalent to (3), so the boundary of the  $\epsilon$ -pseudospectrum is the curve on which  $1/\sigma_1((A - zI)^{-1}) = \epsilon$ , while the left plots of Figures 1–3 show the curves on

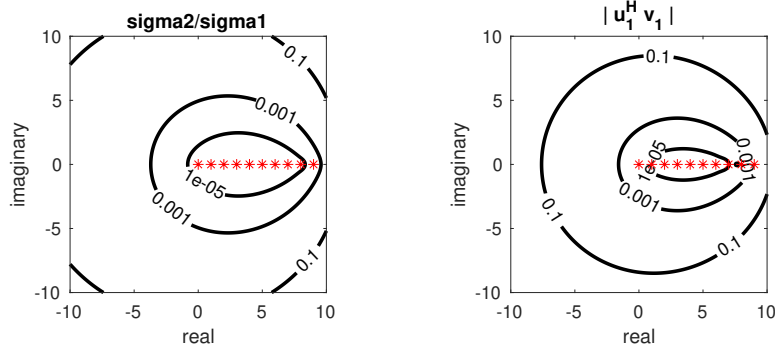


Figure 3: Contour plots of ratios of second largest to largest singular value of the resolvent (left) and of absolute value of inner product of left and right singular vectors corresponding to largest singular value of the resolvent (right). Matrix is the sampling matrix of size  $n = 10$ . Eigenvalues are shown with red asterisks.

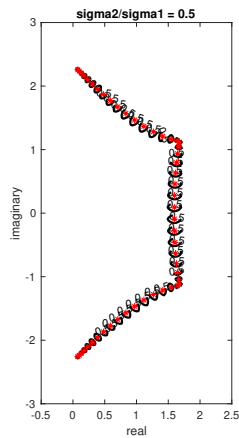


Figure 4: Contour plot of ratios of second largest to largest singular value of the resolvent for a normal matrix with the same eigenvalues as the Grcar matrix of size  $n = 50$ . The 0.5 contour is plotted because contours with much smaller values are barely visible on the scale of the graph. Eigenvalues are shown with red asterisks.

which  $\sigma_2((A - zI)^{-1})/\sigma_1((A - zI)^{-1}) = \epsilon$ , for  $\epsilon = 10^{-5}, 10^{-3}, 10^{-1}$ . In Figure 5, we compare the  $10^{-3}$ -pseudospectrum with the region in which  $\sigma_2((A - zI)^{-1})/\sigma_1((A - zI)^{-1}) < 10^{-3}$  for each of the three matrices in Figures 1–3, as well as for a 10 by 10 Jordan block. For these matrices and for  $z$  in the regions plotted,  $\sigma_2((A - zI)^{-1})$  is not too different from 1, so the curves look similar.

Recall from (2) and (3), however, that there is a difference in scaling between  $S_\epsilon(A)$  and  $\Lambda_\epsilon(A)$ : For a constant  $c$ ,  $S_\epsilon(cA) = cS_\epsilon(A)$  but  $\Lambda_{|c|\epsilon}(cA) = c\Lambda_\epsilon(A)$ . To compare  $S_\epsilon(A)$  to  $\Lambda_\epsilon(A)$ , we should multiply  $A$  by a constant so that, say, the mean value of  $\sigma_2((A - zI)^{-1})$  on  $\Lambda_\epsilon(A)$  is around 1.

To quantify the relation with pseudospectra, we will work with the matrix  $A - zI$ , whose singular values are the inverses of those of  $(A - zI)^{-1}$  and whose right/left singular vectors are the same as the left/right singular vectors of  $(A - zI)^{-1}$ . As noted in item 5 of Theorem 1, the ratio of the smallest to the second smallest singular value of  $A - zI$  is the same as the ratio of the second largest to the largest singular value of  $(A - zI)^{-1}$ . We will use the following inequality,

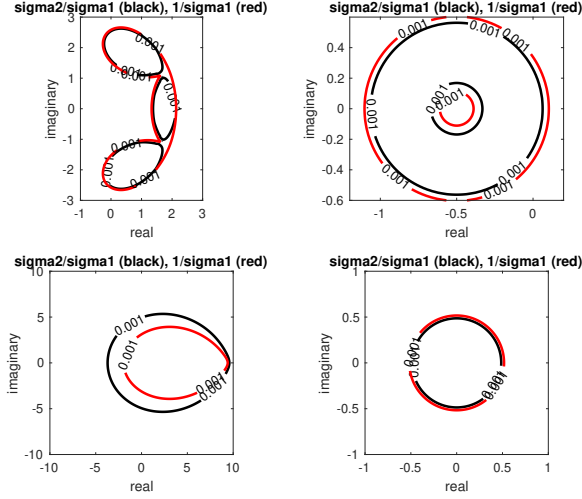


Figure 5: Comparison of curve where  $\sigma_2((A - zI)^{-1})/\sigma_1((A - zI)^{-1}) = 10^{-3}$  (black) to that where  $1/\sigma_1((A - zI)^{-1}) = 10^{-3}$  (red); i.e., to the boundary of the  $10^{-3}$ -pseudospectrum. Upper left is the Gcar matrix of size  $n = 50$ , upper right is the transient\_demo matrix of size  $n = 50$ . Lower left is the sampling matrix of size  $n = 10$ , lower right is a Jordan block of size  $n = 10$ .

which is a consequence of the Wielandt-Hoffman theorem and can be found, for instance, in [Corollary 8.6.2][3]: The decreasingly ordered singular values of two  $n$  by  $n$  matrices  $B$  and  $B + E$  satisfy

$$|\sigma_j(B + E) - \sigma_j(B)| \leq \sigma_1(E). \quad (5)$$

With  $E = -zI$  and  $j = n - 1$ , this implies that

$$\sigma_{n-1}(B) + |z| \geq \sigma_{n-1}(B - zI) \geq \sigma_{n-1}(B) - |z|. \quad (6)$$

This leads to the following theorem relating the  $\epsilon_1$ -pseudospectrum of  $A$  to the region where  $\sigma_2((A - zI)^{-1})/\sigma_1((A - zI)^{-1}) < \epsilon_2$ , for what may be nearby values  $\epsilon_1$  and  $\epsilon_2$ .

**Theorem 2.** *Let  $A$  be an  $n$  by  $n$  matrix with distinct eigenvalues  $\lambda_1, \dots, \lambda_n$ , and let  $\Lambda_\epsilon(A)$  be defined by (3) and  $S_\epsilon(A)$  be defined by (2). Consider the matrices  $A_{0,j} := A - \lambda_j I$ ,  $j = 1, \dots, n$ , each of which has a zero singular value,  $\sigma_n(A_{0,j})$ . Let  $\sigma_{n-1}(A_{0,j}) > 0$  denote the second smallest singular value of  $A_{0,j}$ . For  $r > 1$ ,  $S_{\epsilon(r/((r-1) \min_j \sigma_{n-1}(A_{0,j})))}(A)$  contains*

$$\Lambda_\epsilon(A) \cap \left( \bigcup_{j=1}^n \mathbb{D}(\lambda_j, \sigma_{n-1}(A_{0,j})/r) \right), \quad (7)$$

where  $\mathbb{D}(c, R)$  denotes the open disk about  $c$  of radius  $R$ . In the other direction,

$$S_\epsilon(A) \cap \left( \bigcup_{j=1}^n \mathbb{D}(\lambda_j, \sigma_{n-1}(A_{0,j})/r) \right) \quad (8)$$

is contained in  $\Lambda_{\epsilon((\max_j \sigma_{n-1}(A_{0,j}))((r+1)/r))}(A)$ .

*Proof.* For  $z \in \Lambda_\epsilon(A)$ ,  $\sigma_n(A - zI) < \epsilon$ . From (6), the second smallest singular value of  $A - zI = A_{0,j} - (z - \lambda_j)I$  is greater than or equal to  $\sigma_{n-1}(A_{0,j}) - |z - \lambda_j|$ . Hence for  $z \in \mathbb{D}(\lambda_j, \sigma_{n-1}(A_{0,j})/r)$ ,

the second smallest singular value of  $A - zI$  is greater than  $\sigma_{n-1}(A_{0,j})(r-1)/r$ . It follows that for  $z$  in  $\Lambda_\epsilon(A) \cap \mathbb{D}(\lambda_j, \sigma_{n-1}(A_{0,j})/r)$ , we have  $\sigma_n(A - zI)/\sigma_{n-1}(A - zI) < \epsilon(r/((r-1)\sigma_{n-1}(A_{0,j})))$ . Taking the max over  $j$  of the bounds on  $\sigma_n(A - zI)/\sigma_{n-1}(A - zI)$  establishes (7).

Now suppose  $\sigma_n(A - zI)/\sigma_{n-1}(A - zI) < \epsilon$  and  $z$  lies in one of the disks  $\mathbb{D}(\lambda_j, \sigma_{n-1}(A_{0,j})/r)$ . Then we can write

$$\sigma_n(A - zI) < \epsilon\sigma_{n-1}(A - zI) = \epsilon\sigma_{n-1}(A_{0,j} - (z - \lambda_j)I) \leq \epsilon(\sigma_{n-1}(A_{0,j}) + |z - \lambda_j|) < \epsilon\sigma_{n-1}(A_{0,j})(r+1)/r.$$

Taking the max over  $j$  of the bounds on  $\sigma_n(A - zI)$  establishes (8).  $\square$

If the second smallest singular value of each matrix  $A - \lambda_j I$  is on the order of 1, as it is for the matrices used in Figure 5, and if  $\epsilon$  is small enough so that  $\Lambda_\epsilon(A)$  and  $S_\epsilon(A)$  lie mostly inside the union of disks in (7) and (8), then Theorem 2 establishes a close relationship between pseudospectra and sets where the resolvent is close to a rank one matrix. Taking  $r = 2$ , for example, if  $\min_j \sigma_{n-1}(A_{0,j}) = \max_j \sigma_{n-1}(A_{0,j}) = 1$  and assuming that  $\Lambda_\epsilon(A)$  and  $S_\epsilon(A)$  lie inside the union of disks in (7) and (8), the theorem shows that  $\Lambda_{\epsilon/2}(A) \subset S_\epsilon(A) \subset \Lambda_{(3/2)\epsilon}(A)$  and  $S_{(2/3)\epsilon}(A) \subset \Lambda_\epsilon(A) \subset S_{2\epsilon}(A)$ .

If the second smallest singular value of each matrix  $A_{0,j}$ ,  $j = 1, \dots, n$ , is *not* on the order of 1, then this close relationship may not hold. For example, suppose one starts with the `transient_demo` matrix (whose eigenvalues all have the same condition number), computes an eigendecomposition  $X\Lambda X^{-1}$ , then randomly permutes the diagonal entries of  $\Lambda$  and forms the matrix  $A = X\text{diag}(\lambda_{\pi_1}, \dots, \lambda_{\pi_n})X^{-1}$ . Then  $A$  will have the same eigenvalues with the same condition numbers and the same eigenvectors as the `transient_demo` matrix, the only difference being that different eigenvalues are associated with different eigenvectors. However, the matrices  $A_{0,j} = A - \lambda_j I$  in Theorem 2, are entirely different. In our experiments with  $n = 50$ , the matrices  $A_{0,j}$  had several singular values in the  $10^{-8}$  range. In this case, the sets  $\Lambda_\epsilon(A)$  and  $S_\epsilon(A)$  are entirely different.

## 4 Analysis for a Jordan Block

To understand more about why Figures 1–3 show such large regions of the complex plane where the resolvent,  $(A - zI)^{-1}$ , closely resembles a rank one matrix we will look for disks about the eigenvalues of  $A$  that can be shown to be contained in these regions. Since  $\sigma_n(A - zI) = \min_{w \neq 0} \|(A - zI)w\|/\|w\|$ , one can obtain a good upper bound on  $\sigma_n(A - zI)$  by displaying a vector  $w$  that approximately minimizes this ratio. Here we do this for an  $n$  by  $n$  Jordan block.

**Theorem 3.** *Let  $A$  be an  $n$  by  $n$  Jordan block so that*

$$A - zI = \begin{bmatrix} -z & 1 & & & \\ & \ddots & \ddots & & \\ & & \ddots & 1 & \\ & & & -z & \\ & & & & -z \end{bmatrix}_{n \times n}.$$

*The smallest singular value  $\sigma_n(A - zI)$  is less than or equal to  $|z|^n$ , and the second smallest singular value  $\sigma_{n-1}(A - zI)$  is greater than or equal to  $1 - |z|$ . It follows that for any  $\epsilon \in (0, 1)$ , the set of points  $z$  at which  $\sigma_n(A - zI)/\sigma_{n-1}(A - zI) < \epsilon$  contains a disk about the origin of radius  $r$ , where  $r^n/(1 - r) = \epsilon$ ; this always includes a disk of radius  $\frac{1}{2}\epsilon^{1/n}$ .*

*Proof.* If  $w = [1, z, z^2, \dots, z^{n-1}]^T$ , then  $(A - zI)w = [0, \dots, 0, -z^n]^T$ . Since  $\sigma_n(A - zI) = \min_{w \neq 0} \|(A - zI)w\|/\|w\|$ , it follows that

$$\sigma_n(A - zI) \leq \frac{|z^n|}{\sqrt{\sum_{j=0}^{n-1} |z^j|^2}} \leq |z^n|. \quad (9)$$

The Jordan block  $A$  has a zero singular value and  $n - 1$  ones as singular values, since  $A^H A = \text{diag}(0, 1, \dots, 1)$ . Combining (9) and (6), we see that

$$\sigma_n(A - zI)/\sigma_{n-1}(A - zI) \leq |z|^n/(1 - |z|). \quad (10)$$

It follows that  $z \in S_\epsilon(A)$  if  $|z|^n/(1 - |z|) < \epsilon$ .

Finally, given  $\epsilon \in (0, 1)$ , if  $|z| < \frac{1}{2}\epsilon^{1/n}$ , then  $|z|^n < 2^{-n}\epsilon$  and  $1 - |z| > 1/2$  so that

$$\sigma_n(A - zI)/\sigma_{n-1}(A - zI) < 2^{-(n-1)}\epsilon \leq \epsilon.$$

□

Note that the radius of the black circle in the lower right plot of Figure 5 is about 0.486, and the 10th root of  $10^{-3}$  is about 0.501. Theorem 3 guarantees that  $S_{10^{-3}}(A)$  contains a disk about the origin of radius  $r$ , where  $r^{10}/(1 - r) = 10^{-3}$ , and solving for  $r$  we find  $r \approx 0.470$ .

This can be compared with a known result about the  $\epsilon$ -pseudospectrum of a Jordan block. It is shown in [10] that the  $\epsilon$ -pseudospectrum of an  $n$  by  $n$  Jordan block contains a disk about the origin of radius  $\epsilon^{1/n}$  and is contained in a disk about the origin of radius  $1 + \epsilon$ . The lower bound is demonstrated to be a much sharper estimate of the actual radius.

## 5 Large Toeplitz Matrices

For more general large Toeplitz matrices, results about how close the resolvent is to a rank one (or otherwise low rank) matrix can be derived from what is known as the *splitting phenomenon* [1, Theorem 9.4]. An infinite Toeplitz matrix has the form

$$\begin{bmatrix} a_0 & a_{-1} & a_{-2} & \dots \\ a_1 & a_0 & a_{-1} & \dots \\ a_2 & a_1 & a_0 & \dots \\ \vdots & \vdots & \vdots & \ddots \end{bmatrix},$$

and its *symbol*  $a(t)$  can be defined as a map from the unit circle to the complex plane by

$$a(t) := \sum_{j=-\infty}^{\infty} a_j t^j, \quad \text{where } \sum_{j=-\infty}^{\infty} |a_j| < \infty.$$

We will be interested in symbols  $b(t)$  with only finitely many nonzero Fourier coefficients:

$$b(t) := \sum_{j=-r}^s b_j t^j, \quad t \in \text{unit circle},$$

and we will denote the corresponding infinite Toeplitz matrix as  $T(b)$  and its top  $n$  by  $n$  block as  $T_n(b)$ . Assume that  $b(t) \neq 0$  for all  $t$  on the unit circle, and let  $k$  be the *winding number*



of  $b$ ; i.e., the number of times that  $b(t)$  surrounds the origin in a counterclockwise direction as  $t$  traverses the unit circle. Then, according to the splitting theorem [11], as  $n \rightarrow \infty$ , the  $|k|$  smallest singular values of  $T_n(b)$  approach 0 exponentially, while, for  $n$  sufficiently large, the remaining singular values are bounded away from 0 by a constant  $d > 0$  that depends only on  $b$ .

To determine  $S_\epsilon(T_n(b))$  for  $n$  sufficiently large, we must consider the symbol  $b(t) - z$  and look for values of  $z$  for which the winding number of  $b(t) - z$  about the origin is  $\pm 1$ . The Gröbner matrix, considered previously, is a Toeplitz matrix whose symbol is  $-t^{-1} + 1 + t + t^2 + t^3$ . By result 1 of Theorem 1, we can consider this matrix minus  $2I$ , so that the symbol is  $b(t) = -t^{-1} - 1 + t + t^2 + t^3$ . The image of the unit circle under  $b$  is shown in the upper left plot of Figure 6. Clearly, the absolute value of the winding number of this curve about the origin is 1, and any shift  $z$  such that  $b(t) - z$  still surrounds the origin with winding number  $\pm 1$  will be in  $S_\epsilon(T_n(b))$  for  $n$  sufficiently large since the ratio of the smallest to the second smallest singular value of  $T_n(b) - zI$  will approach 0 as  $n \rightarrow \infty$ . This is illustrated in the upper right and lower left plots of Figure 6, for  $z = 0$  and  $z = -0.5$ . These plots show the smallest (red) and second smallest (black) singular values for  $n = 5$  to 50. The upper right plot is on a linear scale, while the lower left plot uses a log scaling on the vertical axis to clearly show  $\sigma_n(T_n(b) - zI)$  approaching 0 exponentially. It seems clear from the plots that  $\sigma_n(T_n(b) - zI) \rightarrow 0$  as  $n \rightarrow \infty$  and that  $\sigma_{n-1}(T_n(b) - zI)$  approaches a nonzero value as  $n \rightarrow \infty$ . In the lower right plot, we chose a shift  $z = -0.55 - i$ , so that the origin was inside one of the small loops of the shifted symbol. Here the winding number is 2, so the smallest and second smallest singular values of  $T_n(b) - zI$  go to 0 as  $n \rightarrow \infty$ , and it is the third smallest singular value that is bounded away from 0. This is illustrated in the lower right plot of Figure 6. In this case, the splitting theorem does not guarantee that  $z$  will lie in  $S_\epsilon(A)$  for  $n$  sufficiently large, but it appears from the plot that this will be the case since  $\sigma_n(T_n(b) - zI)$  seems to be going to 0 at a faster rate than  $\sigma_{n-1}(T_n(b) - zI)$ .

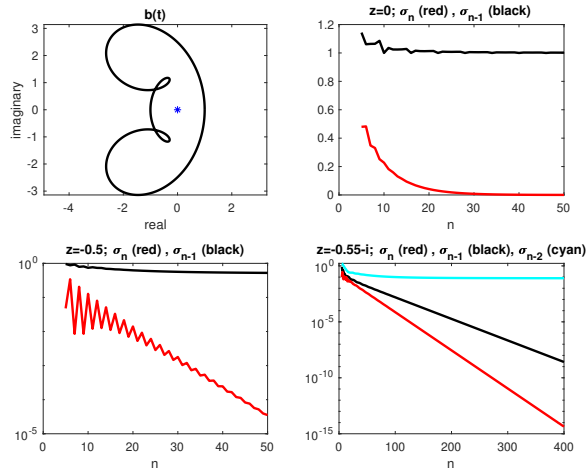


Figure 6: Upper left plot shows image of the unit circle under  $b(t) = -t^{-1} - 1 + t + t^2 + t^3$ . The upper right and lower left plots show the smallest (red) and second smallest (black) singular values of  $T_n(b) - zI$  as a function of  $n$  for  $z = 0$  and  $z = -0.5$ ; for these values, the winding number of  $b(t) - z$  about the origin is 1. Such values lie in  $S_\epsilon(T_n(b))$  for  $n$  sufficiently large. The lower right plot shows the smallest (red), second smallest (black), and third smallest (cyan) singular values of  $T_n(b) - zI$  as a function of  $n$  for  $z = -0.55 - i$ . In this case, the winding number of  $b(t) - zI$  about the origin is 2, so the two smallest singular values go to 0 as  $n \rightarrow \infty$ , while the third smallest singular value remains bounded away from 0.

## 6 More General Analysis

Let  $\lambda$  be a simple eigenvalue of  $A$  and define  $A_0 := A - \lambda I$ . Then  $A_0$  has a zero eigenvalue that is also a zero singular value  $\sigma_n(A_0)$ . The following theorem bounds the growth rate of  $\sigma_n(A_0 - zI)$  with  $|z|$ , based on near-orthogonality properties that may be satisfied by the singular vectors  $u_n$  and  $v_n$  corresponding to the zero singular value of  $A_0$ .

**Theorem 4.** *Let  $\lambda$  be a simple eigenvalue of  $A$  and let  $A_0 := A - \lambda I = U\Sigma V^*$  be a singular value decomposition of  $A_0$ , where  $U := [u_1, \dots, u_n]$ ,  $V := [v_1, \dots, v_n]$ ,  $\Sigma := \text{diag}(\sigma_1, \dots, \sigma_{n-1}, 0)$ ,  $\sigma_1 \geq \dots \geq \sigma_{n-1} > 0$ . Let  $A_0^\dagger$  denote the Moore-Penrose pseudoinverse of  $A_0$ :*

$$A_0^\dagger := V_{n-1}\Sigma_{n-1}^{-1}U_{n-1}^H, \quad (11)$$

where  $U_{n-1} := [u_1, \dots, u_{n-1}]$ ,  $V_{n-1} := [v_1, \dots, v_{n-1}]$ , and  $\Sigma_{n-1} = \text{diag}(\sigma_1, \dots, \sigma_{n-1})$ . For each  $k = 1, 2, \dots$ , the smallest singular value of  $A_0 - zI$  is less than or equal to

$$\left\| \sum_{j=1}^k z^j (u_n^H (A_0^\dagger)^{j-1} v_n) u_n + z^{k+1} (A_0^\dagger)^k v_n \right\| \leq \quad (12)$$

$$|z| \left( \sum_{j=1}^k |z|^{j-1} |u_n^H (A_0^\dagger)^{j-1} v_n| + |z|^k / \sigma_{n-1}^k \right). \quad (13)$$

Assuming that the spectral radius of  $zA_0^\dagger$  is less than one, taking  $k = \infty$  in (12) results in the following upper bound on the smallest singular value of  $A_0 - zI$ :

$$|z| |u_n^H (I - zA_0^\dagger)^{-1} v_n|. \quad (14)$$

*Proof.* Define

$$w := v_n + \sum_{j=1}^k z^j (A_0^\dagger)^j v_n.$$

Then  $\|w\| \geq 1$ , since the range of  $A_0^\dagger$  is orthogonal to  $v_n$ . Since  $A_0 A_0^\dagger = A_0 (V_{n-1} \Sigma_{n-1}^{-1} U_{n-1}^H) = U_{n-1} U_{n-1}^H$ , we can evaluate the product  $(A_0 - zI)w$  term-by-term as:

$$\begin{aligned} (A_0 - zI)w &= (A_0 - zI)v_n + \sum_{j=1}^k \left( z^j U_{n-1} U_{n-1}^H (A_0^\dagger)^{j-1} v_n - z^{j+1} (A_0^\dagger)^j v_n \right) \\ &= -zv_n - \sum_{j=2}^{k+1} z^j (A_0^\dagger)^{j-1} v_n + \sum_{j=1}^k z^j U_{n-1} U_{n-1}^H (A_0^\dagger)^{j-1} v_n \\ &= -\sum_{j=1}^k z^j u_n u_n^H (A_0^\dagger)^{j-1} v_n - z^{k+1} (A_0^\dagger)^k v_n. \end{aligned} \quad (15)$$

The upper bound in (12) is the norm of  $(A_0 - zI)w$ , and that in (13) is obtained by replacing each term in (15) by its norm and noting that the norm of  $(A_0^\dagger)^k v_n$  is less than or equal to  $1/\sigma_{n-1}^k$ .

Assuming that the spectral radius of  $zA_0^\dagger$  is less than one, the quantity  $z^{k+1} (A_0^\dagger)^k v_n$  in (15) will go to 0 as  $k \rightarrow \infty$ , and the summation in (15) becomes  $-z(u_n^H (I - zA_0^\dagger)^{-1} v_n) u_n$ , whose norm is given in (14).  $\square$

Taking  $k = 1$  in (13), we obtain the bound

$$\sigma_n(A_0 - zI) \leq |u_n^H v_n| |z| + |z|^2 / \sigma_{n-1}.$$

If  $\lambda$  is an ill-conditioned eigenvalue, then we know that  $|u_n^H v_n|$  is tiny and if  $\sigma_{n-1} \approx 1$ , then this shows that  $\sigma_n(A_0 - zI)$  grows more like  $|z|^2$  than like  $|z|$  for  $|u_n^H v_n| \ll |z| \ll 1$ . If  $u_n$  is also nearly orthogonal to  $A_0^\dagger v_n$ , then taking  $k = 2$  in (13) suggests that the growth rate of  $\sigma_n(A_0 - zI)$  with  $|z|$  may be more like  $|z|^3$ , and the more powers  $j$  for which  $|u_n^H (A_0^\dagger)^j v_n|$  is small, the higher the power of  $|z|$  describing the growth of  $\sigma_n(A_0 - zI)$ , for  $|z| \ll 1$ . The smallest bound in Theorem 4 may be obtained for  $k = \infty$ , if  $u_n$  is almost orthogonal to  $(I - zA_0^\dagger)^{-1} v_n$ .

Note that the vector  $w$  used in the proof of Theorem 3, namely,  $w = [1, z, z^2, \dots, z^{n-1}]$ , is of the same form as that used in the proof of Theorem 4, since the singular value decomposition of a Jordan block can be written as  $U\Sigma V^H$ , where  $U$  is the identity,  $\Sigma = \text{diag}(1, \dots, 1, 0)$ , and

$$V = \begin{bmatrix} 0 & \dots & 0 & 1 \\ 1 & \dots & 0 & 0 \\ & \ddots & & \vdots \\ & & 1 & 0 \end{bmatrix}.$$

Thus  $v_n$  is the first unit vector,  $u_n$  is the  $n$ th unit vector, and the pseudoinverse is

$$A_0^\dagger = \begin{bmatrix} 0 & 0 & \dots & 0 \\ 1 & 0 & \dots & 0 \\ & \ddots & & \vdots \\ & & 1 & 0 \end{bmatrix}.$$

It follows that  $(A_0^\dagger)^j v_n$  is the  $(j + 1)$ st unit vector, for  $j = 1, \dots, n - 1$  and  $u_n$  is orthogonal to  $(A_0^\dagger)^j v_n$  for  $j = 0, \dots, n - 2$ , while  $u_n^H (A_0^\dagger)^{n-1} v_n = 1$  and  $u_n^H (I - zA_0^\dagger)^{-1} v_n = z^{n-1}$ . In the next section, we will show how the pseudoinverse comes into the derivative of the singular vectors  $v_n$  and  $u_n$ .

In all of the matrices associated with Figures 1–3,  $u_n$  is nearly orthogonal not just to  $v_n$  but also to several powers  $(A_0^\dagger)^j v_n$ . Defining  $A_0$  to be  $(A - \lambda I)$ , where  $\lambda$  is an eigenvalue of  $A$  with maximal condition number, we computed  $\sigma_{n-1}$ ,  $|u_n^H v_n|$ ,  $|u_n^H (A_0^\dagger)^j v_n|$ , and  $|u_n^H (A_0^\dagger)^j v_n| / \|(A_0^\dagger)^j v_n\|$  for  $j = 1, \dots, 5$ . For the Grcar matrix,  $\sigma_{n-1} \approx 0.81$ ,  $|u_n^H v_n| \approx 4.6e - 8$ , and  $|u_n^H (A_0^\dagger)^j v_n|$ ,  $j = 1, \dots, 5$ , ranged from  $1.0e - 7$  to  $5.7e - 3$ ; after dividing by  $\|(A_0^\dagger)^j v_n\|$  to measure the level of orthogonality, the results ranged from  $1.1e - 7$  to  $4.0e - 3$ . For the transient\_demo matrix,  $\sigma_{n-1} \approx 0.18$ ,  $|u_n^H v_n| \approx 1.4e - 6$ , and the values of  $|u_n^H (A_0^\dagger)^j v_n|$  ranged from  $2.7e - 5$  to  $2.5$ , but there was still a significant degree of orthogonality between the vectors, as the values of  $|u_n^H (A_0^\dagger)^j v_n| / \|(A_0^\dagger)^j v_n\|$  ranged from  $5.0e - 6$  to  $4.3e - 3$ . For the sampling matrix,  $\sigma_{n-1} \approx 6.6$ ,  $|u_n^H v_n| \approx 7.6e - 7$ , and the values of  $|u_n^H (A_0^\dagger)^j v_n|$  ranged from  $1.1e - 6$  (for  $j = 2$ ) down to  $7.3e - 8$  (for  $j = 5$ ), but after normalizing, we see that, in addition to  $u_n$  being nearly orthogonal to  $(A_0^\dagger)^j v_n$ , the norms of these vectors decreased with  $j$ ; the range of values for  $|u_n^H (A_0^\dagger)^j v_n| / \|(A_0^\dagger)^j v_n\|$  was  $3.0e - 6$  (for  $j = 1$ ) to  $1.3e - 2$  (for  $j = 5$ ).

**Corollary 5.** *With the notation and assumptions of Theorem 4, let  $\epsilon \in (0, 1)$  be given. The region  $S_\epsilon(A)$  contains the set of points  $z \in \mathbb{C}$  such that  $|z - \lambda| < \sigma_{n-1}$  and the expression in either (12), (13), or (14), with  $z$  replaced by  $(z - \lambda)$ , is bounded above by  $\epsilon(\sigma_{n-1} - |z - \lambda|)$ .*

*Proof.* From Theorem 4,  $\sigma_n(A - zI) = \sigma_n(A_0 - (z - \lambda)I)$  is bounded above by the quantities in (12), (13), and (14), when  $z$  is replaced by  $z - \lambda$  in these expressions. It follows from (6) that  $\sigma_{n-1}(A - zI) = \sigma_{n-1}(A_0 - (z - \lambda)I)$  is bounded below by  $\sigma_{n-1} - |z - \lambda|$ . The result follows since  $\sigma_2((A - zI)^{-1})/\sigma_1((A - zI)^{-1}) = \sigma_{n-1}(A - zI)/\sigma_n(A - zI)$ .  $\square$

Figures 7–9 show the regions about each eigenvalue where

$$\min_{k=1,\dots,100} |z - \lambda| \left( \sum_{j=1}^k |z - \lambda|^{j-1} |u_n^H(A_0^\dagger)^{j-1} v_n| + |z - \lambda|^k / \sigma_{n-1}^k \right) \leq 10^{-3}(\sigma_{n-1} - |z - \lambda|), \quad (16)$$

and where

$$|z - \lambda| |u_n^H(I - (z - \lambda)(A_0^\dagger)^{-1} v_n)| \leq 10^{-3}(\sigma_{n-1} - |z - \lambda|), \quad (17)$$

for the Grcar matrix, the transient\_demo matrix and the sampling matrix. Note that inequality (16) describes disks about each eigenvalue (outlined in blue in the figures) since it depends only on  $|z - \lambda|$ , while inequality (17) describes more general regions (outlined in green). The disks outlined in blue cover a good portion of  $S_{10^{-3}}(A)$ , and the regions outlined in green cover still more of  $S_{10^{-3}}(A)$ .

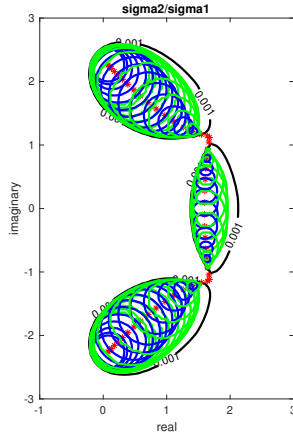


Figure 7: Disks about each eigenvalue where inequality (16) is satisfied (outlined in blue) and regions about each eigenvalue where inequality (17) is satisfied (outlined in green).  $S_{10^{-3}}(A)$  is outlined in black. Matrix is the Grcar matrix of size  $n = 50$ .

Theorem 4 also leads to a new result about pseudospectra:

**Corollary 6.** *With the notation and assumptions of Theorem 4, let  $\epsilon > 0$  be given. The  $\epsilon$ -pseudospectrum contains the set of points  $z \in \mathbb{C}$  such that the expression in (12), (13), or (14), with  $z$  replaced by  $z - \lambda$ , is bounded above by  $\epsilon$ .*

*Proof.* From Theorem 4,  $\sigma_n(A - zI) = \sigma_n(A_0 - (z - \lambda)I)$  is bounded above by the expressions in (12), (13), and (14), when  $z$  is replaced by  $z - \lambda$  in these expressions. The result follows since  $1/\sigma_1((A - zI)^{-1}) = \sigma_n(A - zI)$ .  $\square$

The regions defined in Corollary 6 come even closer to filling the  $\epsilon$ -pseudospectrum of  $A$ . We illustrate this just for the Grcar matrix in Figure 10. Interestingly, each of the regions outlined in green, where  $|z - \lambda| |u_n^H(I - (z - \lambda)(A_0^\dagger)^{-1} v_n)| \leq 10^{-3}$ , contains a large portion of  $\Lambda_{10^{-3}}(A)$ , and not just a region around the eigenvalue  $\lambda$ .

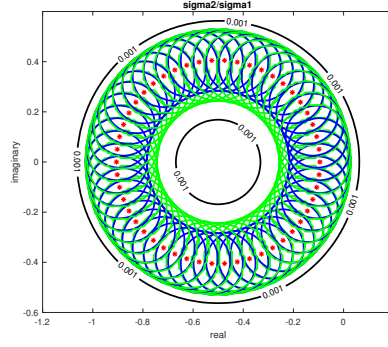


Figure 8: Disks about each eigenvalue where inequality (16) is satisfied (outlined in blue) and regions about each eigenvalue where inequality (17) is satisfied (outlined in green).  $S_{10-3}(A)$  is outlined in black. Matrix is the transient\_demo matrix of size  $n = 50$ .

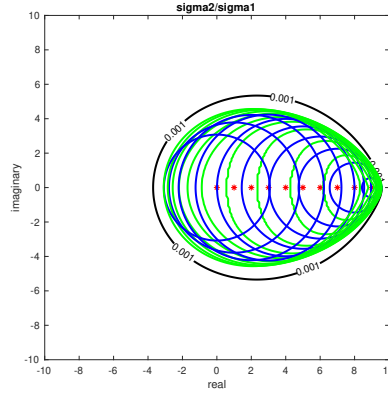


Figure 9: Disks about each eigenvalue where inequality (16) is satisfied (outlined in blue) and regions about each eigenvalue where inequality (17) is satisfied (outlined in green).  $S_{10-3}(A)$  is outlined in black. Matrix is the sampling matrix of size  $n = 10$ .

## 7 Differentiation of Singular Values and Singular Vectors

In the previous section, we described regions where  $\sigma_2((A - zI)^{-1})/\sigma_1((A - zI)^{-1}) < \epsilon$ . We now wish to consider regions where  $|u_n(z)^H v_n(z)| < \epsilon$ , where  $u_n(z)$  and  $v_n(z)$  are right and left singular vectors associated with the largest singular value of  $(A - zI)^{-1}$ , that is, with the smallest singular value of  $A - zI$ . It was noted in Section 2 that these regions appear to be slightly smaller.

In general, the SVD is *not* continuously differentiable unless singular values are allowed to become negative [7, 2, 16]. However, one can differentiate in one direction, provided there are no multiple singular values (and, in some cases, even if there are multiple singular values) [8]. Therefore, let us fix  $\theta \in [0, 2\pi)$ , set  $A(r) := A_0 - r e^{i\theta} I$ ,  $r \geq 0$ , where  $A_0$  has a simple eigenvalue 0 that is also a singular value, and write the SVD of  $A(r)$  as  $A(r) = U(r)\Sigma(r)V(r)^H$ . Then

$$A'(r) = -e^{i\theta} I = U'(r)\Sigma(r)V(r)^H + U(r)\Sigma'(r)V(r)^H + U(r)\Sigma(r)(V'(r))^H. \quad (18)$$

We also require  $U(r)^H U(r) = V(r)^H V(r) = I$ , and differentiating these equations leads to

$$(U'(r))^H U(r) + U(r)^H U'(r) = (V'(r))^H V(r) + V(r)^H V'(r) = 0. \quad (19)$$

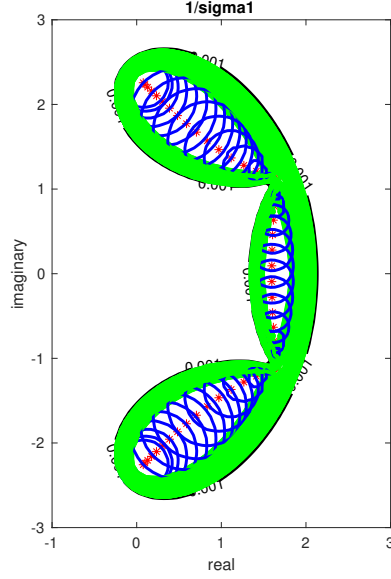


Figure 10: Disks about each eigenvalue derived from inequality (13) (outlined in blue) and regions about each eigenvalue derived from inequality (14) (outlined in green) that lie in the  $10^{-3}$ -pseudospectrum (outlined in black). Matrix is the Grcar matrix of size  $n = 50$ .

Multiplying (18) on the left by  $U(r)^H$  and on the right by  $V(r)$  leads to the relation

$$-e^{i\theta}U(r)^H V(r) = U(r)^H U'(r)\Sigma(r) + \Sigma'(r) + \Sigma(r)(V'(r))^H V(r). \quad (20)$$

Equating real parts of the diagonal entries in (20) and noting that equation (19) says that  $U(r)^H U'(r)$  and  $(V'(r))^H V(r)$  are skew Hermitian so that the real parts of their diagonal entries are zero, we find

$$-\text{Re}(e^{i\theta} \text{diag}(U(r)^H V(r))) = \text{diag}(\Sigma'(r)). \quad (21)$$

Thus the derivative of  $\sigma_n(r)$  is

$$\sigma'_n(r) = -\text{Re}(e^{i\theta} u_n(r)^H v_n(r)), \quad (22)$$

showing that a small inner product  $|u_n(r)^H v_n(r)|$  between left and right singular vectors leads to slow change in the singular value  $\sigma_n(r)$ . Conversely, if one can establish that  $\sigma_n(r)$  changes slowly with  $r$  in all directions, then this would imply that  $|u_n(r)^H v_n(r)|$  must be small; unfortunately, in previous sections we have established only upper bounds on  $\sigma_n(r)$ , leaving open the possibility that it might alternate quickly between 0 and these upper bounds.

Defining  $Z(r) := U(r)^H U'(r)$  and  $W(r) := V(r)^H V'(r)$  and equating imaginary parts of the diagonal entries in (20) leads to  $n$  equations in  $2n$  unknowns:

$$-i \text{Im}(e^{i\theta} \text{diag}(U(r)^H V(r))) = \text{diag}(Z(r))\Sigma(r) + \Sigma(r)\text{diag}(W(r)^H). \quad (23)$$

Any solution to these equations, say, taking  $\text{diag}(Z(r)) = \text{diag}(W(r)^H)$  should lead to the same result that  $A(r) = U(r)\Sigma(r)V(r)^H$ , where  $U(r)^H U(r) = V(r)^H V(r) = I$ . Note, however, that if  $\sigma_n(0) = 0$ , then these equations have no solution unless  $\text{Im}(e^{i\theta} u_n(0)^H v_n(0)) = 0$ . In this case, we can replace any computed  $u_n(0)$  by  $e^{i\varphi} u_n(0)$ , where  $\varphi = \theta + \arg(u_n(0)^H v_n(0)) + \pi$  so that  $\sigma'_n(0) = -\text{Re}(e^{i\theta} u_n(0)^H v_n(0))$  will be nonnegative.

Equating the  $n^2 - n$  off-diagonal entries in (20) and using the fact that  $Z(r)$  and  $W(r)$  are skew Hermitian, we can solve for  $Z(r)$  and  $W(r)$ . Define  $Q(r) := U(r)^H A'(r) V(r) = -e^{i\theta} U(r)^H V(r)$ . Dropping the argument  $r$  for convenience, and looking at the  $(j, k)$  and  $(k, j)$  entries of (20), we find

$$\begin{aligned}\sigma_k z_{jk} + \sigma_j \bar{w}_{kj} &= Q_{jk}, \\ \sigma_j z_{kj} + \sigma_k \bar{w}_{jk} &= Q_{kj}.\end{aligned}\tag{24}$$

Substituting  $z_{kj} = -\bar{z}_{jk}$  and  $\bar{w}_{jk} = -w_{kj}$ , the second equation becomes

$$\sigma_j \bar{z}_{jk} + \sigma_k w_{kj} = -Q_{kj},$$

and taking complex conjugates

$$\sigma_j z_{jk} + \sigma_k \bar{w}_{kj} = -\overline{Q_{kj}}.\tag{25}$$

Assuming that  $\sigma_j \neq \sigma_k$ , equations (24) and (25) now enable us to solve for  $z_{jk}$  and  $\bar{w}_{kj}$ , say, for  $j < k$  and we use the fact that these matrices are skew-Hermitian to set the rest of their off-diagonal entries. To see what to do in case  $\sigma_j = \sigma_k$ , see [16]. Finally, after solving for  $Z(r)$  and  $W(r)$ , we get  $U'(r) = U(r)Z(r)$  and  $V'(r) = V(r)W(r)$ .

We are interested in the quantity  $u_n(r)^H v_n(r)$ , whose derivative is  $(u'_n(r))^H v_n(r) + u_n(r)^H v'_n(r)$ . Since  $u'_n(r) = U(r)z_n(r)$ , where  $z_n(r)$  is the  $n$ th column of  $Z(r)$  and  $v'_n(r) = V(r)w_n(r)$ , where  $w_n(r)$  is the  $n$ th column of  $W(r)$ , we can use formulas (24) and (25) with  $k = n$  and  $j < n$ , along with the formulas  $Q_{jn} = -e^{i\theta} u_j^H v_n$  and  $Q_{nj} = -e^{i\theta} u_n^H v_j$ , to solve for the relevant quantities. Again dropping the argument  $r$  for convenience, we can write

$$z_{jn} = -(e^{i\theta} \sigma_n u_j^H v_n + e^{-i\theta} \sigma_j v_j^H u_n) / (\sigma_n^2 - \sigma_j^2),\tag{26}$$

$$\bar{w}_{nj} = (e^{-i\theta} \sigma_n v_j^H u_n + e^{i\theta} \sigma_j u_j^H v_n) / (\sigma_n^2 - \sigma_j^2).\tag{27}$$

Since  $W$  is skew Hermitian,

$$w_{jn} = -(e^{-i\theta} \sigma_n v_j^H u_n + e^{i\theta} \sigma_j u_j^H v_n) / (\sigma_n^2 - \sigma_j^2).\tag{28}$$

It follows that

$$\begin{aligned}v_n^H u'_n = v_n^H U z_n &= v_n^H \left[ \sum_{j=1}^{n-1} \frac{e^{i\theta} \sigma_n (u_j^H v_n) + e^{-i\theta} \sigma_j (v_j^H u_n)}{\sigma_j^2 - \sigma_n^2} u_j + z_{nn} u_n \right] \\ &= e^{i\theta} \sigma_n \sum_{j=1}^{n-1} \frac{|u_j^H v_n|^2}{\sigma_j^2 - \sigma_n^2} + e^{-i\theta} \sum_{j=1}^{n-1} \sigma_j \frac{(v_j^H u_n)(v_n^H u_j)}{\sigma_j^2 - \sigma_n^2} + z_{nn} v_n^H u_n.\end{aligned}\tag{29}$$

When  $r = 0$ , the first term in (29) is 0 since  $\sigma_n(0) = 0$ . The third term involves  $z_{nn}(0)$ , but based on the argument after (23), we can take  $z_{nn}(0) = 0$ . Thus we are left with only the second term in (29), which can be written in the form

$$e^{-i\theta} v_n^H U_{n-1} \Sigma_{n-1}^{-1} V_{n-1}^H u_n = e^{-i\theta} v_n^H (A_0^\dagger)^H u_n,$$

where again the pseudoinverse  $A_0^\dagger$  is involved. Thus

$$(u'_n(0))^H v_n(0) = e^{i\theta} u_n(0)^H A_0^\dagger v_n(0).\tag{30}$$

Similarly, we can write

$$\begin{aligned}
u_n^H v_n' &= u_n^H V w_n = u_n^H \left[ \sum_{j=1}^{n-1} \frac{e^{-i\theta} \sigma_n (v_j^H u_n) + e^{i\theta} \sigma_j (u_j^H v_n)}{\sigma_j^2 - \sigma_n^2} v_j + w_{nn} v_n \right] \\
&= e^{-i\theta} \sigma_n \sum_{j=1}^{n-1} \frac{|v_j^H u_n|^2}{\sigma_j^2 - \sigma_n^2} + e^{i\theta} \sum_{j=1}^{n-1} \sigma_j \frac{(u_j^H v_n)(u_n^H v_j)}{\sigma_j^2 - \sigma_n^2} + w_{nn} u_n^H v_n. \quad (31)
\end{aligned}$$

Again for  $r = 0$ , the first term in (31) is 0 since  $\sigma_n(0) = 0$ , and the third term is 0 since  $w_{nn}(0)$  can be taken to be 0. Again we are left with the second term in (31), which can be written as

$$e^{i\theta} u_n^H V_{n-1} \Sigma_{n-1}^{-1} U_{n-1}^H v_n = e^{i\theta} u_n^H A_0^\dagger v_n.$$

Thus

$$u_n(0)^H v_n'(0) = e^{i\theta} u_n(0)^H A_0^\dagger v_n(0). \quad (32)$$

Combining (30) and (32), we see that

$$\left. \frac{d}{dr} (u_n(r)^H v_n(r)) \right|_{r=0} = 2e^{i\theta} u_n(0)^H A_0^\dagger v_n(0). \quad (33)$$

Again the quantity  $u_n(0)^H A_0^\dagger v_n(0)$  is related to the rate of change of  $u_n(r)^H v_n(r)$  with  $r$ , as it was related to the rate of change of  $\sigma_n(A_0 - zI)$  in Theorem 4. If  $|u_n(0)^H A_0^\dagger v_n(0)|$  is tiny then we expect  $|u_n(r)^H v_n(r)|$  to grow (or decay) more like  $r^2$  than like  $r$ , for small  $r$ . Unfortunately, higher derivatives of  $u_n(r)^H v_n(r)$  are significantly more complicated, and we do not have a result analogous to that in Corollary 5 describing a region where  $|u_n(r)^H v_n(r)| < \epsilon$ . This remains an open problem.

## 8 Some Possible Applications and Remaining Open Problems

A number of applications, most notably in fluid mechanics, involve working with large resolvent matrices [9, 12, 14], and it has been observed, based on physical grounds, that it may be sufficient to work with a rank one or low rank approximation to the resolvent. (For some plots of singular values of such resolvents, see [6, 13].) When a large resolvent matrix can be replaced by a rank one or low rank matrix, this results in a huge savings in storage and compute time. In this paper, we have used a different rank one approximation to  $(A - zI)^{-1}$  for each  $z$ , but if the same low rank approximation can be used for many different values of  $z$ , then further savings is possible.

In [4], it was observed that two upper bounds on the norm of an analytic function  $f(A)$  turned out to be approximately the same because the numerical range of the resolvent was close to a disk about the origin; this led to the realization that the resolvent resembled a rank one matrix  $\sigma_1(z) u_1(z) v_1(z)^H$ , where  $u_1(z)$  and  $v_1(z)$  are almost orthogonal to each other. With more knowledge of the behavior of the singular vectors  $u_1(z)$  and  $v_1(z)$ , one might be able to say more about the sharpness, or lack thereof, of these bounds on  $\|f(A)\|$ .

It is surprising that, to the best of our knowledge, the connection between pseudospectra and regions where the resolvent is close to a rank one matrix has not been explained before. The proof just rests on the fact that if the second smallest singular value of the matrices  $A_{0,j}$  in Theorem 2 is on the order of 1, then from (6), the second smallest singular value of  $A_{0,j} - zI$  is between  $1 - |z|$  and  $1 + |z|$ .



In Theorem 4, we do not know how to relate the properties that  $u_n$  be almost orthogonal to  $(A_0^\dagger)^j v_n$  to other standard matrix properties. The property that  $u_n$  be almost orthogonal to  $v_n$  just corresponds to  $\lambda$  being ill-conditioned since the condition number of  $\lambda$  is  $1/|u_n^H v_n|$ . We also do not know for what class of matrices these additional near orthogonality properties hold. They hold for the test problems presented in this paper and for many others that we have tried, but identifying this class of matrices remains an open problem.

Finally, we still have not delineated the region where  $|u_1(z)^H v_1(z)| < \epsilon$ , although in the plots, it appears to be most of  $S_\epsilon(A)$ . Identifying this region remains an open problem.

**Acknowledgments.** The first author thanks Mark Embree for helpful discussions, especially the suggestion to look at Toeplitz matrices. The authors thank the University of Washington Applied Math Department for hosting the sabbatical visit of the second and third authors, during which time this work began.

## References

- [1] A. BÖTTCHER AND S. GRUDSKY, *Spectral Properties of Banded Toeplitz Matrices*, SIAM, 2005.
- [2] A. BUNSE-GERSTNER, R. BYERS, V. MEHRMANN, AND N. NICHOLS, *Numerical computation of an analytic singular value decomposition of a matrix valued function*, Numer. Math. 60, pp. 1-39, 1991.
- [3] G. GOLUB AND C. VAN LOAN, *Matrix Computations*, 4th edition, Johns Hopkins University Press, 2013.
- [4] A. GREENBAUM AND N. WELLEN, *Comparison of  $K$ -Spectral Set Bounds on Norms of Functions of a Matrix or Operator*, Lin. Alg. Appl. 694, pp. 52-77, 2024.
- [5] R. A. HORN AND C. R. JOHNSON, *Topics in Matrix Analysis*, Cambridge University Press, USA, 1991.
- [6] R. ISLAM AND Y. SUN *Identification of cross-frequency interactions in compressible cavity flow using harmonic resolvent analysis*, 10.48550/arXiv.2406.07705.
- [7] B. DE MOOR AND S. BOYD, *Analytic properties of singular values and vectors*, ESAT-SISTA report 1989-28.
- [8] K. O'NEIL, *Critical points of the singular value decomposition*, SIAM J. Matrix Anal. Appl. 27, pp. 459-473, 2005.
- [9] E. PICKERING, A. TOWNE, P. JORDAN, AND T. COLONIUS, *Resolvent-based modeling of turbulent jet noise*, J. Acoustic Soc. Am., 2021.
- [10] L. REICHEL AND L. N. TREFETHEN, *Eigenvalues and pseudo-eigenvalues of Toeplitz matrices*, Lin. Alg. Appl. 162-164 (1992), pp. 153–185.
- [11] S. ROCH AND B. SILBERMANN *Limiting sets of eigenvalues and singular values of Toeplitz matrices*, Asymptotic Anal., 8, pp. 293-309, 1994.
- [12] L. ROLANDI, J. RIBEIRO, C.A. YEH, AND K. TAIRA *An invitation to resolvent analysis*, Theor. Comput. Fluid Dyn. 38, pp. 603-639, 2024.

- [13] S. SYMON *Reconstruction and estimation of flows using resolvent analysis and data assimilation*, 10.13140/RG.2.2.16136.26885.
- [14] S. SYMON, A. MADHUSUDANAN, S. ILLINGWORTH, AND I. MARUSIC, *Use of eddy viscosity in resolvent analysis of turbulent channel flow*, Phys. Rev. Fluids 8, pp. 1-26, 2023.
- [15] L. N. TREFETHEN AND M. EMBREE, *Spectra and Pseudospectra: The Behavior of Non-normal Matrices and Operators*, Princeton University Press, Princeton and Oxford, 2005.
- [16] K. WRIGHT, *Differential equations for the analytic singular value decomposition of a matrix*, Numer. Math. 63, pp. 283-295, 1992.
- [17] T. M. WRIGHT, M. EMBREE, *EigTool: a graphical tool for nonsymmetric eigenproblems*, <http://www.cs.ox.ac.uk/pseudospectra/eigtool/>.